coatings

MDPI

Article

Influence of Spraying Process Parameters on the Characteristics of Steel Coatings Produced by Arc Spraying Method

Bauyrzhan Rakhadilov [1,2], Nurtoleu Magazov [3,*], Dauir Kakimzhanov [2], Akbota Apsezhanova [3,4], Yermakhan Molbossynov [2,3] and Aidar Kengesbekov [3,5]

1 Surface Engineering and Tribology Research Center, Sarsen Amanzholov East Kazakhstan University, Ust-Kamenogorsk 070002, Kazakhstan; rakhadilovb@gmail.com
2 PlasmaScience LLP, Ust-Kamenogorsk 070010, Kazakhstan; dauir_97@mail.ru (D.K.); molbossynov.ye@edu.ektu.kz (Y.M.)
3 Protective and Functional Coatings Scientific Center, Daulet Serikbayev East Kazakhstan Technical University, Ust-Kamenogorsk 070010, Kazakhstan; akbotaapsezhanova@gmail.com (A.A.); kenesbekovaidar@gmail.com (A.K.)
4 INNOTECHMASH Engineering Center, Ust-Kamenogorsk 070010, Kazakhstan
5 Institute of Composite Materials LLP, Ust-Kamenogorsk 070010, Kazakhstan
* Correspondence: magazovn@gmail.com; Tel.: +7-747-426-3019

Abstract: Arc spraying is one of the most effective and cost-efficient thermal spraying technologies for creating high-quality protective coatings. This paper examines the influence of arc spraying process parameters on the properties of steel coatings. The parameters varied in this study included gas pressure, wire feed rate, and the distance from the spray gun to the substrate (standoff distance). Experimental evaluations focused on surface roughness, thickness, porosity, structure, and hardness of the coatings. The techniques used for these evaluations included profilometry for roughness measurement, scanning electron microscopy (SEM) for structural analysis, Vickers hardness testing, and optical microscopy. The results demonstrate a significant influence of arc spraying parameters on the characteristics of the resulting coatings. The analysis revealed that the coatings produced under different modes exhibit a layered structure and vary in thickness. A detailed examination of the coating structure identified defects such as unmelted particles, voids, and delamination in the interface zone. The study of coating thickness and porosity showed that increasing the wire feed rate and decreasing the standoff distance leads to the formation of thicker and denser coatings. Specifically, increasing the wire feed rate from 2 to 12 cm/s resulted in a decrease in porosity from 12.59% to 4.33% and an increase in coating thickness to 699 µm. The surface analysis highlighted the importance of a comprehensive approach to selecting the optimal roughness. While increasing the wire feed rate up to 12 cm/s can increase the Ra roughness parameter, gas pressure also significantly influences this parameter, reducing roughness from Ra = 18.63 µm at 6 MPa to Ra = 15.95 µm at 8 MPa. Additionally, it was found that varying the arc spraying parameters affects the hardness of the coatings, with all modes resulting in hardness values higher than that of the substrate. Therefore, optimizing these parameters enables the achievement of the best combination of mechanical and structural properties in the coatings. These findings can be valuable for further improvement of arc spraying technologies and the expansion of their application across various industries.

Keywords: arc spraying; steel coatings; microstructure; Vickers hardness; porosity; thickness

Citation: Rakhadilov, B.; Magazov, N.; Kakimzhanov, D.; Apsezhanova, A.; Molbossynov, Y.; Kengesbekov, A. Influence of Spraying Process Parameters on the Characteristics of Steel Coatings Produced by Arc Spraying Method. *Coatings* **2024**, *14*, 1145. https://doi.org/10.3390/coatings14091145

Academic Editor: Ainhoa Riquelme

Received: 31 July 2024
Revised: 1 September 2024
Accepted: 3 September 2024
Published: 5 September 2024

1. Introduction

In mechanical engineering, thermal spraying is one of the key methods for applying protective coatings that are widely used across various industries [1]. This method offers the ability to create coatings with specific characteristics tailored to the needs of particular applications. Various thermal spraying techniques exist, including detonation spraying [2–4], arc spraying [5,6], plasma spraying [7,8], HVOF [9,10], and cold spraying [11,12]. Each

of these processes has distinct characteristics and applications, but arc spraying remains one of the earliest and most widely utilized technologies. It was invented by Max Ulrich Schupp in 1918, gained commercial recognition in the 1960s, and continues to be used in industry due to its high economic efficiency, low equipment and operating costs, and high deposition rates and thermal efficiency [13,14].

Arc spraying, also known as twin-wire arc or electric arc spraying (EAS), is a process in which two electrically conductive wires of opposite polarity are fed through guide rollers to meet at a specific point [15]. At this point, an arc is formed, melting the wires. The molten particles are then accelerated towards the substrate by compressed air or nitrogen, where they solidify or sinter together to form a protective coating.

Arc spraying allows for the production of coatings with high physical and mechanical properties. However, achieving optimal coating quality requires consideration of numerous factors that influence its characteristics. Key parameters include microstructure, fatigue strength, wear rate, corrosion resistance, coating porosity, hardness, strength, deposition efficiency, adhesion strength, surface roughness, and oxide content [16,17]. The final properties of the coating are significantly affected by various parameters of the thermal arc spraying process. These parameters include voltage, current, wire feed rate, standoff distance (SoD), nozzle geometry, coating environment (inert, ambient, or vacuum chamber), spray gas pressure, initial material, gas type (air or nitrogen), substrate surface preheating, and subsequent thermal treatment of the coating lamellae [6,18–23]. Surface preparation methods, such as shot peening and sandblasting, also play a crucial role.

Numerous studies have confirmed the importance of optimizing thermal spraying parameters to achieve the desired characteristics of metallic coatings. For example, Arif et al. [17] examined the influence of standoff distance (SoD) on the properties of brass coatings applied to low-carbon steel, finding that increases in voltage and SoD result in higher surface roughness and alterations in the coatings' microstructure, while deposition efficiency (DE) significantly decreased. Another study [24] explored the characteristics of steel coatings under varying carrier gas pressure, standoff distance, and torch power, revealing that coating density increases with higher carrier gas pressure and a reduced SoD. Johnston et al. [23] demonstrated that spraying parameters impact the microstructure, porosity, and hardness of zinc coatings. Kumar et al. [25] optimized the parameters for twin-wire arc spraying of aluminum coatings, while Kumar and Pandey [26] showed how plasma spraying parameters influence coating thickness and surface roughness. However, improper selection of EAS parameters can lead to high porosity, increased oxide content, low DE, and high surface roughness [27,28]. This underscores the necessity of optimizing EAS parameters to produce effective coatings tailored for specific applications [29].

A considerable amount of literature addresses the EAS process. However, most studies focus on materials such as zinc, chromium, aluminum, and brass, while steel coatings, particularly those made from 30KhGSA steel, are less extensively studied. This type of steel is frequently used in environments requiring protection from abrasive and erosive wear, making it a promising candidate for various applications in mechanical engineering. Therefore, the primary objective of this study was to investigate the characteristics of 30KhGSA steel coatings produced by arc spraying. The study varied key process parameters, such as gas pressure, wire feed rate, and the distance from the spray gun to the sample surface. The coatings were evaluated based on surface roughness, thickness, porosity, microstructure, and hardness. The discussion focuses on determining optimal parameters to better understand the arc spraying process of steel wires and their influence on coating properties.

2. Materials and Methods

2.1. Description of the Equipment Used

Arc spraying (AS) is a process in which a jet of molten metal droplets is formed by the action of a fast-moving gas on the continuously melting tips of consumable wires. These wires are fed into a direct current arc that is formed between the wires. This process

provides effective spraying and deposition of molten particles on the substrate surface, resulting in the formation of a protective coating with high performance characteristics.

The coatings were applied using the SX-600 supersonic electric arc metallizer, manufactured by Guangzhou Sanxin Metal S&T Co., Ltd. (Guangzhou, China). The system comprises a power supply, a supersonic sprayer, a control system, and a compressed air system. The power supply ensures a stable voltage necessary for maintaining a consistent spraying process. The control system allows for the regulation of the wire feed rate and electrical parameters during spraying. The compressed air system controls the gas pressure, which directly influences the quality and uniformity of the spray.

The wire spraying was conducted according to the settings outlined in Table 1. The parameters in the specified modes were varied by adjusting factors such as gas pressure (P), wire feed rate (V), and the distance from the spray gun to the sample surface (SoD). The voltage during the spraying process was maintained at 42 $\pm$ 3 V. Air was used as the spraying gas. Each sample was sprayed across the entire substrate surface to obtain an even layer within 10 s. The ambient temperature was controlled within the range of 27–29 °C, and the humidity was kept constant throughout the entire series of experiments.

Table 1. Spraying regimes.

Sample	P, MPa	V, cm/s	D, mm
V1	9	2	200
V2	9	4	200
V3	9	8	200
V4	9	12	200
D1	9	12	100
D2	9	12	150
D3	9	12	200
D4	9	12	250
P1	6	12	200
P2	7	12	200
P3	8	12	200
P4	9	12	200

Each sample obtained is labeled according to the parameters to be changed. Samples labeled V refer to a change in the wire feed rate parameter. Samples labeled D refer to a change in the SoD. Samples labeled P refer to a change in the gas pressure parameter.

2.2. Characteristics of Materials Used and Sample Preparation

The coatings were sprayed on prepared substrates of 65G steel. This is a high-carbon spring steel with high wear resistance and good mechanical properties, making it an excellent choice for high-load and friction applications. The chemical composition of the substrate is shown in Table 2.

Table 2. Chemical composition of 65G steel substrate.

Fe, wt%	C, wt%	Si wt%	Mn wt%	Ni wt%	S wt%	P wt%	Cr wt%	Cu wt%
base	0.62–0.7	0.17–0.37	0.9–1.2	up to 0.25	up to 0.035	up to 0.035	up to 0.25	up to 0.2

Before spraying, the surface of the substrates was thoroughly prepared by sandblasting. Sandblasting was performed using electrocorundum, which was fed from a gun through a nozzle with a diameter of 5 mm under air pressure of 7 MPa. Such treatment allows effective removal of oxides, contaminants, and roughness from the substrate surface, providing better adhesion of the sprayed coating to the substrate.

As coating material, 30KhGSA steel-grade wire was used. This is an alloyed structural steel characterized by high strength and wear resistance due to the presence of chromium, silicon, and manganese in its composition. The chemical composition of the steel wire is shown in Table 3. The diameter of the wire was 14 mm.

Table 3. Chemical composition of 30KhGSA steel.

Fe, wt%	C, wt%	Si wt%	Mn wt%	Ni wt%	S wt%	P wt%	Cr wt%	Cu wt%
base	0.28–0.34	0.9–1.2	0.8–1.1	up to 0.3	up to 0.025	up to 0.025	0.8–1.1	up to 0.3

2.3. Methods for Evaluating the Characteristics of Coatings

To investigate the structure and porosity of the coatings, cross sections of the samples were prepared. The samples were processed using standard sectioning methods, followed by grinding and mechanical polishing. Grinding was performed using SiC abrasive papers with grit sizes ranging from 120 to 3000, and polishing was carried out with velvet cloth and diamond paste on an automatic polishing machine, model METAPOL 2200P (Laizhou Lyric Testing Equipment Co., Shandong, China). Microstructure analysis was conducted using a Tescan Vega 4 scanning electron microscope (Tescan, Brno, Czech Republic). Prior to analysis, the samples were mounted on special conductive tape. The examination was conducted at an accelerating voltage of 20 kV. To analyze coating porosity, images were captured at selected magnifications using an Olympus BX53M optical microscope (Olympus, Tokyo, Japan). Porosity was calculated according to ASTM E2109 using metallographic analysis software. Test method B, which involves automatic image analysis in the software, was employed. To minimize errors, at least 10 separate areas were analyzed. The average coating thickness was measured based on five measurements for each coating image. Surface roughness was evaluated using the contact profilometry method with a Profilometer 130 (Proton, Zelenograd, Russia). Five measurements were taken at random locations on each coated sample to ensure result reproducibility and minimize errors, followed by recalculation of numerical values according to GOST 2789-73. Adhesion tests were carried out on an Elcometer 510 T pull-off adhesion tester (Elcometer, Manchester, UK) with 20 mm dollies. Microhardness was also analyzed. Vickers microhardness testing was performed using a semiautomatic microhardness tester, Metolab 502 (Metolab, St. Petersburg, Russia), in accordance with GOST-2999-75. A minimum of 10 measurements were taken at random points to determine the microhardness.

3. Results

3.1. Microstructure

SEM images revealed that the coatings produced by arc spraying exhibited a similar layered structure across all processing modes. Figure 1 presents the structure of the sample produced under a working gas pressure of 9 MPa, a wire feed rate of 12 cm/s, and an SoD of 200 mm (D3 sample), illustrating the characteristic layered morphology observed in other conditions as well. During the spraying process, molten particles ejected from the metallizer reach the substrate surface, where they rapidly cool and solidify, forming thin layers or lamellae [30,31]. This rapid cooling facilitates the formation of the layered structure. Each layer consists of a solidified particle or group of particles that accumulate on top of one another.

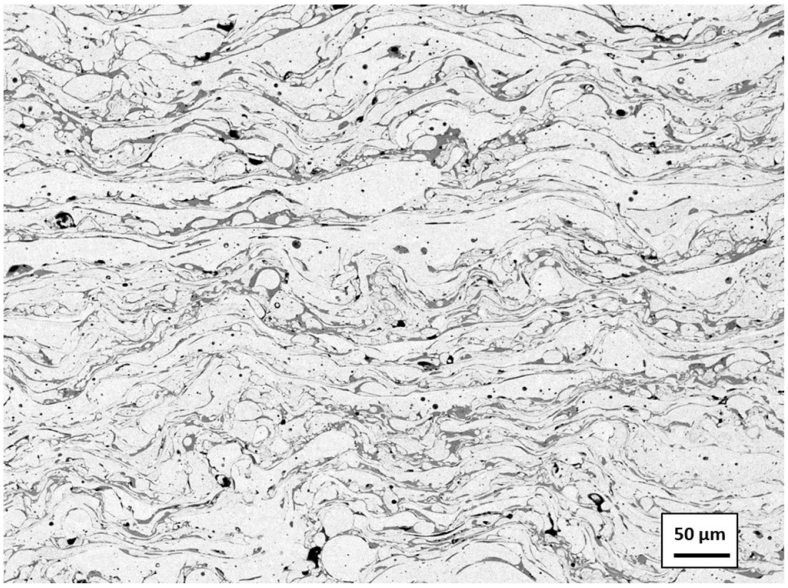

Figure 1. Typical layered microstructure of the cross section of the coatings (D3 sample).

It was observed that the structure comprises both light and dark regions. Figure 2 shows the structure of the sample produced under a wire feed rate of 8 cm/s, a working gas pressure of 9 MPa, and an SoD of 200 mm (V3 sample). A mixture of light and dark regions is evident, with alternating lamellae of both phases present in all samples. Additionally, rounded light phases are visible within the dark regions. The dark regions exhibit cracks within their structure, whereas the light regions do not. Furthermore, the light regions appear to hinder the propagation of cracks originating from the dark regions (Figure 2). Similar findings were reported in studies investigating the microstructural characteristics of steel coatings produced by twin-wire arc spraying [24].

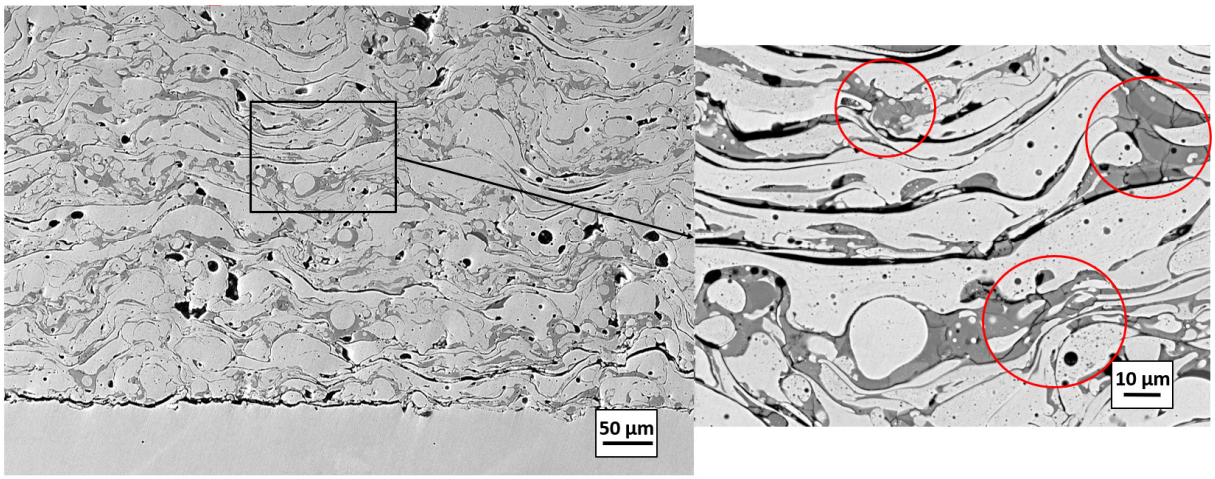

Figure 2. Microstructure of V3 coating with alternating light and dark zones (red circles highlight cracks in dark zones).

The investigation also revealed zones with defects such as pores, delaminations, and unmelted particles within the coating structure at various depths. For instance, Figure 3 presents the microstructure of sample D4, highlighting the identified defects. Pores (Figure 3, marked in red as 1) can form due to gas or air entrapment, inadequate fusion of molten particles, or improper regulation of spraying parameters (e.g., gas pressure or temperature). The numerical data on porosity variation as a function of spraying parameters are discussed in Section 3.2 of this article. Delaminations between the coating

lamellae (Figure 3, marked in green as 2), as well as at the interface, are also evident. These delaminations may result from insufficient bonding between layers or between the coating and the substrate. Another observed defect is unmelted particles (Figure 3, marked in blue as 3). These are material particles that did not fully melt during the spraying process and remained on the substrate or between lamellae in a solid state. Unmelted particles can compromise coating adhesion and may serve as initiation points for microcracks and other defects.

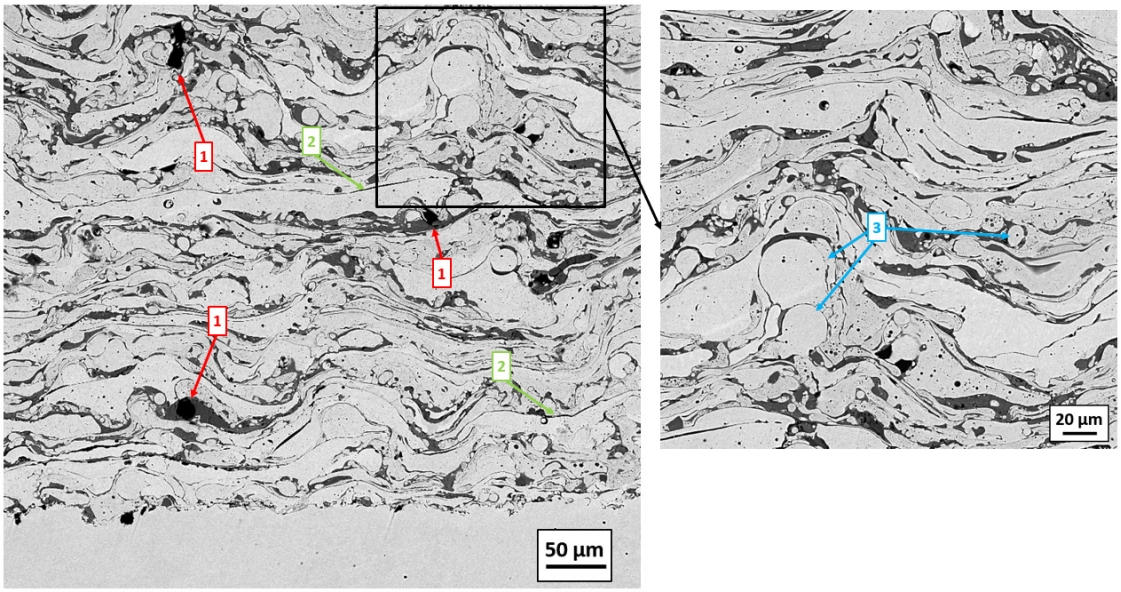

Figure 3. Microstructural analysis of the D4 coating with detection of defect zones (designations: 1—pores, 2—delaminations, 3—unmelted particles).

The influence of various process parameters on defect formation is clearly evident in the SEM graphs. Figure 4 presents coatings obtained at different gas pressure levels, emphasizing how changes in gas pressure affect the microstructure of the coatings, particularly in terms of defect formation. For instance, at a higher gas pressure of 9 MPa (P4 coating), the micrograph reveals a significant increase in defects, such as delaminations and unmelted particles, compared to the coating applied at 7 MPa (P2 coating). In contrast, the coating applied at 7 MPa exhibits fewer defects, resulting in a more uniform and robust structure, which correlates with higher hardness values.

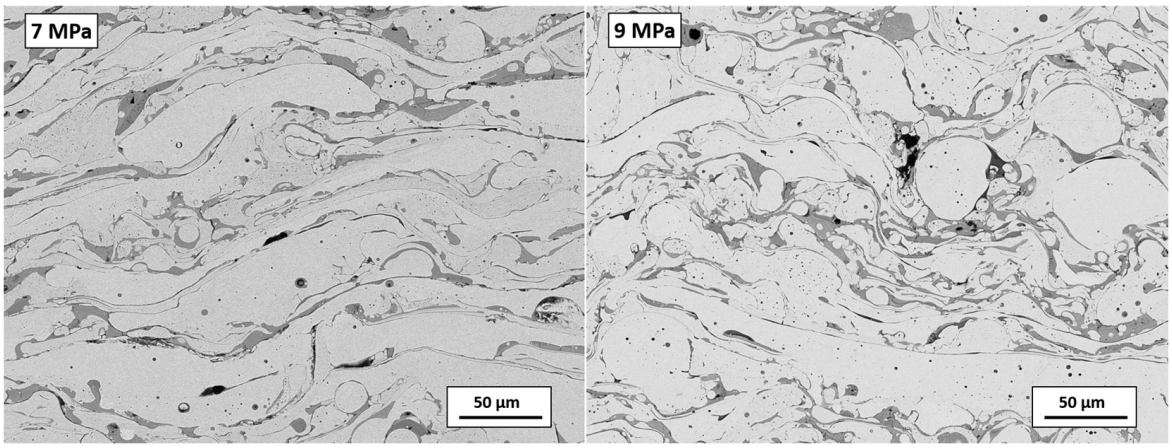

Figure 4. The influence of gas pressure on defect formation throughout the coating depth.

3.2. Thickness and Porosity

Thickness and porosity of coatings are two of the main properties characterizing coatings [32]. The thickness and porosity of coatings depending on the variation of parameters were investigated.

The effect of wire feed rate on the thickness of the coatings demonstrates a direct relationship: as the wire feed rate increases, the coating thickness also increases (Figure 5). The porosity of the coatings decreases with increasing wire feed rate, reaching minimum values of 8.38% and 4.33% at 8 and 12 cm/s, respectively. An increase in wire feed rate raises the amount of sprayed material, contributing to greater coating thickness. Additionally, the increased material deposition can result in denser coatings. This increased material density enhances surface coverage, thereby reducing the number of pores and voids in the coating. Moreover, as the wire feed rate increases, more particles impact the surface, which can compact the layers already applied. This compaction further reduces the porosity of the coating.

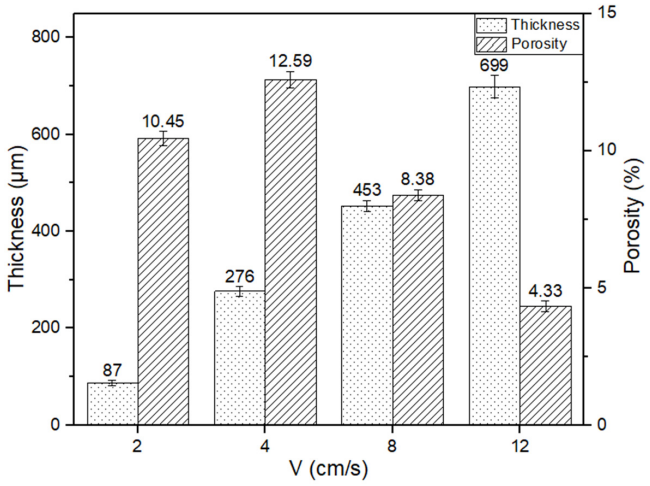

Figure 5. Dependence of coating thickness and porosity on wire feed rate.

The study of the influence of working gas pressure (Figure 6) shows that the maximum thickness values of 712 and 699 microns were achieved for samples produced at 7 and 9 MPa, respectively. The minimum porosity values were also observed in samples processed at 7 and 9 MPa. These gas pressures are the most optimal for producing thick and dense coatings.

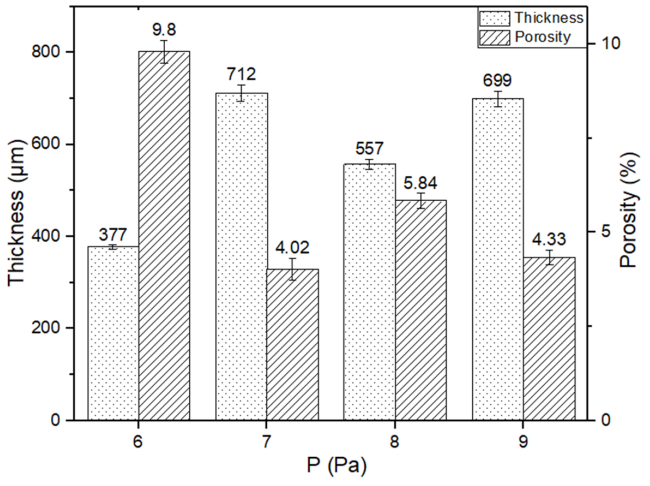

Figure 6. Dependence of coating thickness and porosity on gas pressure.

At shorter distances, the coating thickness was greater (Figure 7). The thickest coating among all samples was obtained at an SoD of 150 mm. However, as the SoD increased, the coating thickness decreased. Thus, it can be concluded that an SoD of 150 mm is optimal for achieving thicker coatings, which could reduce operating costs by requiring less metallization work while using the same amount of wire. However, the porosity study revealed that coatings sprayed at lower SoD values (100 and 150 mm) exhibited relatively high porosity. In contrast, increasing the SoD to 200 mm led to a reduction in porosity and the formation of denser coatings. Further increasing the SoD from 200 to 250 mm resulted in a twofold decrease in thickness, along with a sharp increase in porosity to the highest values observed among all samples. Therefore, a further increase in SoD was not deemed reasonable.

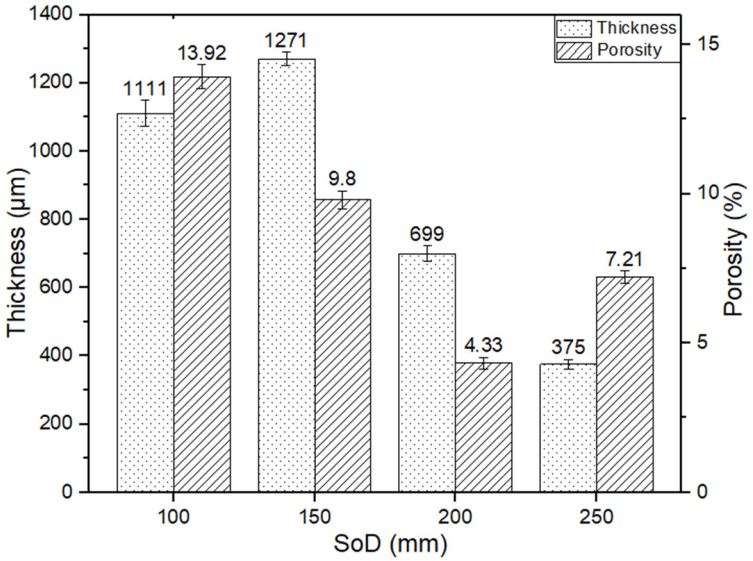

Figure 7. Dependence of coating thickness and porosity on standoff distance.

3.3. Surface Roughness and Adhesion

The R_a parameter (arithmetic mean deviation of the profile) was chosen as the main parameter to describe roughness. This parameter defines the arithmetic mean of absolute values of profile deviations from the center line within the base length. Therefore, further in the text, when we say "roughness", we mean this parameter.

The results obtained by varying each parameter are shown in Figure 8. It can be observed that changes in spraying parameters lead to different ranges of surface roughness (Ra) values. Decreasing each parameter to its minimum value, such as 2 cm/s for wire feed rate (V), 100 mm for SoD, and 6 MPa for gas pressure, results in an increase in roughness within these ranges. When the wire feed rate is increased, Ra decreases to a minimum of 12.45 µm at 4 cm/s. However, further increases in the wire feed rate lead to an increase in roughness, with values of 13.96 and 17.05 µm observed at 8 and 12 cm/s, respectively. This increase in roughness can be attributed to the rise in arc current and the quantity of sprayed material, which results in the deposition of larger particles [23].

Varying the gas pressure (P) produced the widest range of roughness values. The lowest roughness values, 16.74 and 15.95 µm, were obtained at gas pressures of 7 and 8 MPa, respectively. However, increasing the gas pressure to a maximum of 9 MPa resulted in an increase in roughness to 17.05 µm.

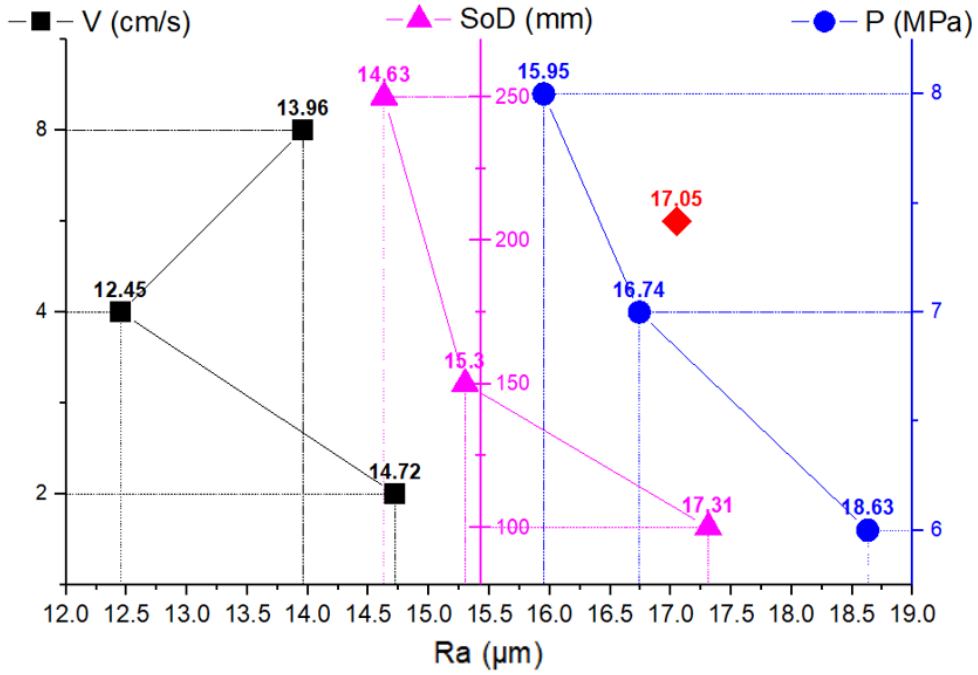

Figure 8. Change in coating roughness depending on spraying parameters (V—wire feed rate, SoD—distance from gun to substrate surface, P—gas pressure, red diamond is the common regime for all parameters).

Regarding SoD, high and similar roughness values were observed at distances of 100 and 200 mm. At SoD values of 150 and 250 mm, a decrease in roughness was noted. Varying the SoD alters the velocity–temperature relationship of the particles. In thermal spraying, an optimal SoD should allow the particles sufficient time to melt, ensuring a dense coating; however, an excessively large SoD may cause the molten particles to solidify before reaching the substrate [21]. Conversely, reducing the SoD may increase particle velocity upon impact with the substrate, leading to coatings with uniformity, high density, and low roughness [33]. Therefore, finding the optimal SoD values is crucial.

The adhesion strength of the coatings was evaluated using the pull-off method in accordance with ASTM D4541. For this purpose, dollies were bonded to the coating surface using a universal high-strength adhesive, ensuring optimal contact and reliable adhesion to the surface. After the adhesive had fully cured, a perpendicular force was applied to the dolly until the coating detached from the substrate. During the experiment, a maximum force of 25 MPa was recorded, after which no further increase in force occurred and the device reached its operational limit. This indicates that the adhesion strength of the coating exceeded the capabilities of the equipment used. We are currently preparing to conduct additional adhesion tests using alternative methods that will allow for a more precise evaluation of the adhesion strength. The results of these tests are planned to be published in a subsequent article.

3.4. Vickers Hardness

The microhardness of the coatings strongly depends on the coating spraying modes. The results are summarized in Table 4.

Table 4. Mechanical properties of the coatings.

P, MPa	V, cm/s	D, mm	HV
9	**2**	200	316.2 ± 22
9	**4**	200	377 ± 21
9	**8**	200	404 ± 22
9	**12**	**200**	327.1 ± 19
9	12	**100**	280.8 ± 12
9	12	**150**	340.7 ± 15
9	12	**250**	334.5 ± 20
6	12	200	326.5 ± 16
7	12	200	392.6 ± 9
8	12	200	343.8 ± 22
	initial		250.3 ± 6

The microhardness of the initial material is 250.3 HV, which is significantly lower than the microhardness of the coatings produced under various spraying conditions. This underscores the effectiveness of the arc spraying process in enhancing the mechanical properties of surfaces. At a pressure of 9 MPa and a distance of 200 mm, increasing the wire feed rate from 2 to 8 cm/s leads to an increase in coating microhardness from 316.2 to 404 HV. However, a further increase in the feed rate to 12 cm/s results in a decrease in microhardness to 327.1 HV. At a feed rate of 12 cm/s and different pressures (6, 7, 8, 9 MPa), the maximum microhardness is achieved at 7 MPa, reaching 392.6 ± 9 HV. The highest microhardness (404 HV) is obtained at a wire feed rate of 8 cm/s, a pressure of 9 MPa, and a distance of 200 mm. This suggests that there is an optimal combination of spraying parameters that yields the highest mechanical properties. Conversely, the lowest microhardness (280.8 HV) is observed when the pressure is varied and the distance is reduced.

The selection of optimal process parameters is crucial for achieving high mechanical properties. For instance, non-optimal spraying conditions, such as a wire feed rate of 2 cm/s, result in the formation of porous and thin coatings with low hardness. A thin coating with a thickness of 87 μm and a porosity of 10.45% exhibits one of the lowest hardness values (316.2 ± 22 HV). This confirms that high porosity and insufficient thickness can significantly diminish the strength characteristics of the coating. However, as demonstrated by the sample at an SoD of 100 mm, even a considerable coating thickness (1111 μm) coupled with high porosity (13.92%) leads to a significant reduction in hardness to 280.8 ± 12 HV. This indicates that coating hardness may depend not only on thickness and porosity but also on other defects.

For a deeper understanding of the influence of various parameters on coating hardness, consider the comparison of samples with varying gas pressures (7 and 9 MPa). Despite similar porosity (4.33% and 4.02%) and coating thickness (699 and 712 μm), the hardness of these coatings differs significantly. The coating applied at 7 MPa exhibits a hardness of 392.6 ± 9 HV, which is notably higher than the 327.1 ± 19 HV observed at 9 MPa. This finding confirms that even with similar porosity and thickness, hardness can vary significantly depending on the presence of other defects. As discussed in Section 3.1 (Figure 4), the coating applied at 9 MPa, although denser, has a more defective structure, including delaminations and unmelted particles. These defects reduce the overall strength of the coating, which explains the observed differences in hardness.

Adjusting each of the arc spraying parameters, such as wire feed rate, distance, and gas pressure, leads to significant changes in coating microhardness, highlighting the importance of a comprehensive approach to optimizing these parameters for achieving optimal properties.

4. Conclusions

This study demonstrated that varying arc spraying parameters, such as gas pressure, wire feed rate, and standoff distance (SoD), has a significant impact on the characteristics of the resulting coatings. Experimental studies confirmed that adjusting these parameters leads to changes in surface roughness, thickness, porosity, structure, and hardness of the coatings. The key findings of the study are as follows.

1. Increasing the wire feed rate from 2 to 12 cm/s leads to an increase in coating thickness to 699 μm and a significant reduction in porosity to 4.33%. However, further increasing the speed to 12 cm/s can increase the surface roughness. The hardness of the coating increases as the wire feed rate is raised from 2 to 8 cm/s, reaching 404 HV. However, a further increase to 12 cm/s results in a decrease in hardness.
2. The optimal SoD for achieving a thicker coating is 150 mm, while a denser coating is achieved at 200 mm. However, increasing the SoD to 250 mm results in a significant decrease in coating thickness and an increase in porosity. The lowest hardness of the coating, 280 HV, is observed at an SoD of 100 mm, highlighting the importance of accurately selecting the SoD to achieve the best mechanical properties.
3. The maximum thickness and minimum porosity values of the coatings are achieved at gas pressures of 7 and 9 MPa, indicating that these pressures are optimal for producing dense coatings. Gas pressure has a significant effect on the surface roughness, reducing it from Ra = 18.63 μm at 6 MPa to Ra = 15.95 μm at 8 MPa. The maximum hardness of the coating is achieved at a pressure of 7 MPa, emphasizing the need for precise pressure control to obtain the best mechanical properties.

Based on the experimental data, it was found that to obtain a coating of 30KhGSA steel with high physical and mechanical characteristics, the following technological conditions for arc spraying should be applied: a working gas pressure of 9 MPa, a wire feed rate of 12 cm/s, and an SoD of 200 mm; alternatively, a pressure of 7 MPa, a wire feed rate of 12 cm/s, and an SoD of 200 mm. These parameters yield optimal coating thickness, minimal porosity, and high coating hardness. However, to further improve the technology and validate the results, additional experiments are planned to test other combinations of parameters, including a wire feed rate of 8 cm/s, an SoD of 150 mm, and a gas pressure of 8 MPa, to determine the most optimal parameters for different operating conditions.

Author Contributions: Conceptualization, B.R. and N.M.; methodology, D.K. and A.K.; formal analysis, N.M. and D.K.; investigation, Y.M., D.K. and A.A.; writing—original draft preparation, N.M. and Y.M.; writing—review and editing, B.R. and A.K.; supervision, B.R. and N.M.; project administration, B.R. and N.M.; funding acquisition, B.R. All authors have read and agreed to the published version of the manuscript.

Funding: This research was funded by the Committee of Science of the Ministry of Science and Higher Education of the Republic of Kazakhstan (grant BR21882370).

Institutional Review Board Statement: Not applicable.

Informed Consent Statement: Not applicable.

Data Availability Statement: Data is contained within the article.

Conflicts of Interest: Authors Bauyrzhan Rakhadilov, Dauir Kakimzhanov and Yermakhan Molbossynov were employed by PlasmaScience LLP. Author Aidar Kengesbekov was employed by Institute of Composite Materials LLP. The remaining authors declare that the research was conducted in the absence of any commercial or financial relationships that could be construed as a potential conflict of interest.

References

1. Ramezani, M.; Mohd Ripin, Z.; Pasang, T.; Jiang, C.-P. Surface Engineering of Metals: Techniques, Characterizations and Applications. *Metals* **2023**, *13*, 1299. [CrossRef]
2. Rakhadilov, B.; Maulet, M.; Abilev, M.; Sagdoldina, Z.; Kozhanova, R. Structure and Tribological Properties of Ni–Cr–Al-Based Gradient Coating Prepared by Detonation Spraying. *Coatings* **2021**, *11*, 218. [CrossRef]
3. Rakhadilov, B.; Sulyubayeva, L.; Maulet, M.; Sagdoldina, Z.; Buitkenov, D.; Issova, A. Investigation of High-Temperature Oxidation of Homogeneous and Gradient Ni-Cr-Al Coatings Obtained by Detonation Spraying. *Coatings* **2023**, *14*, 11. [CrossRef]
4. Rakhadilov, B.; Kantay, N.; Sagdoldina, Z.; Erbolatuly, D.; Bektasova, G.; Paszkowski, M. Experimental Investigations of Al_2O_3- and ZrO_2-Based Coatings Deposited by Detonation Spraying. *Mater. Res. Express* **2021**, *8*, 056402. [CrossRef]
5. Bobzin, K.; Wietheger, W.; Burbaum, E.; Johann, L.M. High-Velocity Arc Spraying of Fe-Based Metallic Glasses with High Si Content. *J. Therm. Spray Tech.* **2022**, *31*, 2219–2228. [CrossRef]
6. Gargasas, J.; Valiulis, A.V.; Gedzevičius, I.; Mikaliūnas, Š.; Nagurnas, S.; Pokhmurska, H. Optimization of the Arc Spraying Process Parameters of the Fe–Base Mn-Si-Cr-Mo-Ni Coatings for the Best Wear Performance. *Mater. Sci.* **2016**, *22*, 20–24. [CrossRef]
7. Rakhadilov, B.K.; Kenesbekov, A.B.; Kowalevski, P.; Ocheredko, Y.A.; Sagdoldina, Z.B. Development of Air-Plasma Technology for Hardening Cutting Tools by Applying Wear-Resistant Coatings. *News Natl. Acad. Sci. Repub. Kazakhstan Ser. Geol. Tech. Sci.* **2020**, *3*, 54–62. [CrossRef]
8. Zhu, H.; Li, D.; Yang, M.; Ye, D. Prediction of Microstructure and Mechanical Properties of Atmospheric Plasma-Sprayed 8YSZ Thermal Barrier Coatings Using Hybrid Machine Learning Approaches. *Coatings* **2023**, *13*, 602. [CrossRef]
9. Rakhadilov, B.; Muktanova, N.; Kakimzhanov, D.; Satbayeva, Z.; Kassenova, L.; Magazov, N. Investigation of the Influence of Powder Fraction on Tribological and Corrosion Characteristics of 86WC-10Co-4Cr Coating Obtained by HVOF Method. *Coatings* **2024**, *14*, 651. [CrossRef]
10. Górnik, M.; Jonda, E.; Łatka, L.; Nowakowska, M.; Godzierz, M. Influence of Spray Distance on Mechanical and Tribological Properties of HVOF Sprayed WC-Co-Cr Coatings. *Mater. Sci.-Pol.* **2021**, *39*, 545–554. [CrossRef]
11. Winnicki, M.; Łatka, L.; Jasiorski, M.; Baszczuk, A. Mechanical Properties of TiO2 Coatings Deposited by Low Pressure Cold Spraying. *Surf. Coat. Technol.* **2021**, *405*, 126516. [CrossRef]
12. Winnicki, M. Advanced Functional Metal-Ceramic and Ceramic Coatings Deposited by Low-Pressure Cold Spraying: A Review. *Coatings* **2021**, *11*, 1044. [CrossRef]
13. Fauchais, P. 2-Current Status and Future Directions of Thermal Spray Coatings and Techniques. In *Future Development of Thermal Spray Coatings*; Espallargas, N., Ed.; Woodhead Publishing: Sutton, UK, 2015; pp. 17–49. ISBN 978-0-85709-769-9.
14. Fantozzi, D.; Matikainen, V.; Uusitalo, M.; Koivuluoto, H.; Vuoristo, P. Chlorine-Induced High Temperature Corrosion of Inconel 625 Sprayed Coatings Deposited with Different Thermal Spray Techniques. *Surf. Coat. Technol.* **2017**, *318*, 233–243. [CrossRef]
15. Rakhadilov, B.; Shynarbek, A.; Kakimzhanov, D.; Kusainov, R.; Zhassulan, A.; Ormanbekov, K. Effect of Voltage on Properties of 30HGSA Steel Coatings by Supersonic Supersonic Arc Metallization Method. *Adv. Sci. Technol. Res. J.* **2024**, *18*, 113–124. [CrossRef]
16. Kumar, S.; Kumar, R. Influence of Processing Conditions on the Properties of Thermal Sprayed Coating: A Review. *Surf. Eng.* **2021**, *37*, 1339–1372. [CrossRef]
17. Arif, Z.U.; Shah, M.; Rehman, E.U.; Tariq, A. Effect of Spraying Parameters on Surface Roughness, Deposition Efficiency, and Microstructure of Electric Arc Sprayed Brass Coating. *Int. J. Adv. Appl. Sci.* **2020**, *7*, 25. [CrossRef]
18. Mykhailo, S.; Volodymyr, G.; Oleksandra, S.; Olegas, P.; Pavlo, M.; Olena, O.; Liudmyla, T. The Effect of Increasing the Air Flow Pressure on the Properties of Coatings During the Arc Spraying of Cored Wires. *Stroj. Časopis-J. Mech. Eng.* **2019**, *69*, 133–146. [CrossRef]
19. Abedini, A.; Pourmousa, A.; Chandra, S.; Mostaghimi, J. Effect of Substrate Temperature on the Properties of Coatings and Splats Deposited by Wire Arc Spraying. *Surf. Coat. Technol.* **2006**, *201*, 3350–3358. [CrossRef]
20. Planche, M.P.; Liao, H.; Coddet, C. Relationships between In-Flight Particle Characteristics and Coating Microstructure with a Twin Wire Arc Spray Process and Different Working Conditions. *Surf. Coat. Technol.* **2004**, *182*, 215–226. [CrossRef]
21. Kar, S.; Bandyopadhyay, P.P.; Paul, S. Effect of Arc–Current and Spray Distance on Elastic Modulus and Fracture Toughness of Plasma-Sprayed Chromium Oxide Coatings. *Friction* **2018**, *6*, 387–394. [CrossRef]
22. Hall, A.; McCloskey, J.; Johnston, A. Process-Microstructure Relationships in the Twin Wire Arc Zinc Process. In Proceedings of the 2012 International Thermal Spray Conference, Houston, TX, USA, 20–24 May 2012; Lima, R.S., Agarwal, A., Hyland, M.M., Lau, Y.-C., Li, C.-J., McDonald, A., Toma, F.-L., Eds.; pp. 479–484.
23. Johnston, A.L.; Hall, A.C.; McCloskey, J.F. Effect of Process Inputs on Coating Properties in the Twin-Wire Arc Zinc Process. *J. Therm. Spray Tech.* **2013**, *22*, 856–863. [CrossRef]
24. Wagner, N. Effect of Process Parameters on Twin Wire Arc Sprayed Steel Coatings. *J. Mater. Eng. Perform* **2021**, *30*, 6650–6655. [CrossRef]
25. Kumar, D.; Murtaza, Q.; Singh, R.C. Sliding Wear Behavior of Aluminum Alloy Coating Prepared by Two-Wire Electric Arc Spray Process. *Int. J. Adv. Manuf. Technol.* **2016**, *85*, 237–252. [CrossRef]
26. Kumar, D.; Pandey, K. Optimization of the Process Parameters in Generic Thermal Barrier Coatings Using the Taguchi Method and Grey Relational Analysis. *Proc. Inst. Mech. Eng. Part L J. Mater. Des. Appl.* **2017**, *231*, 600–610. [CrossRef]

27. Arizmendi-Morquecho, A.; Campa-Castilla, A.; Leyva-Porras, C.; Aguilar Martinez, J.A.; Vargas Gutiérrez, G.; Moreno Bello, K.J.; López López, L. Microstructural Characterization and Wear Properties of Fe-Based Amorphous-Crystalline Coating Deposited by Twin Wire Arc Spraying. *Adv. Mater. Sci. Eng.* **2014**, *2014*, 836739. [CrossRef]
28. Boulos, M.I.; Fauchais, P.L.; Heberlein, J.V.R. Wire Arc Spraying. In *Thermal Spray Fundamentals: From Powder to Part*; Boulos, M.I., Fauchais, P.L., Heberlein, J.V.R., Eds.; Springer International Publishing: Cham, Switzerland, 2021; pp. 467–517. ISBN 978-3-030-70672-2.
29. Yao, H.H.; Zhou, Z.; Wang, Y.M.; He, D.Y.; Bobzin, K.; Zhao, L.; Öte, M.; Königstein, T. Microstructure and Properties of FeCrB Alloy Coatings Prepared by Wire-Arc Spraying. *J. Therm. Spray Tech.* **2017**, *26*, 483–491. [CrossRef]
30. Shukla, R.K.; Patel, V.; Kumar, A. Modeling of Rapid Solidification with Undercooling Effect During Droplet Flattening on a Substrate in Coating Formation. *J. Therm. Spray Tech.* **2018**, *27*, 269–287. [CrossRef]
31. Lahmar-Mebdoua, Y.; Vardelle, A.; Fauchais, P.; Gobin, D. Heat Diffusion in Solidifying Alumina Splat Deposited on Solid Substrate under Plasma Sprayed Conditions: Application to Coating Formation. *Defect Diffus. Forum* **2010**, *297–301*, 46–51. [CrossRef]
32. Zhang, S.D.; Zhang, W.L.; Wang, S.G.; Gu, X.J.; Wang, J.Q. Characterisation of Three-Dimensional Porosity in an Fe-Based Amorphous Coating and Its Correlation with Corrosion Behaviour. *Corros. Sci.* **2015**, *93*, 211–221. [CrossRef]
33. Wielage, B.; Wank, A.; Rupprecht, C. *Tailoring of Wire Feedstock and Processing Conditions in High Velocity Combustion Wire Spraying*; Marple, B.R., Hyland, M.M., Lau, Y.-C., Lima, R.S., Voyer, J., Eds.; ASM International: Seattle, WD, USA, 2006; pp. 1009–1014.